LAMINAR MIXED CONVECTION HEAT TRANSFER IN ENCLOSURE WITH PIN FIN HEAT SINKS

Luiz Carlos Cordeiro Jr, lcordeir@hotmail.com
Universidade do Estado do Rio de Janeiro-Resende-RJ - Brazil

Mauricio Araujo Zanardi, mzanardi@feg.unesp.br
UNESP – Universidade Estadual Paulista – Departamento de Energia - Campus of Guaratinguetá

Abstract. *A computational modeling for simulating flow and heat transfer considering the laminar mixed convection inside an enclosure was presented. As a heat source, a pin-fin array was attached to a heating component and this set was mounted at one enclosure vertical wall. Effects of the aspect ratio, the dissipated heat and the injected mass were investigated. The Nusselt number, based on the overall heat transfer coefficient, was determined as a function of the dissipated heat, expressed by the Rayleigh number, and the mass flow rate represented by the Richardson number. The results show, as expected, that the mixed convection enhances the heat transfer mainly for low aspect ratio enclosures. However, for higher aspect ratios, the formation of a recirculation cell at the enclosure top forces the component to operate in higher temperatures than those for pure natural convection.*

Keywords*: Mixed convection, pin-fin heat sink, discrete heat sources in enclosures*

1. INTRODUCTION

The heat transfer in enclosures has been widely studied due to its application on electronic packages cooling. In this kind of application, the use of fin arrays is very suitable to enhance natural convection heat transfer. The analysis and design of finned array heat sinks can be found in many literature sources such as in Kraus and Bar-Cohen (1995).

Natural convection in enclosures with discrete sources, considering the source size and positioning, is a subject that recently has been studied by many researchers. Deng (2002) presented a numerical analysis considering a 2D model for an enclosure with two discrete sources and concluded that the heat transfer was more effective when the source is placed in the lower part of the enclosure. Calcagni et al. (2005) explored the source size effects on the heat transfer coefficient. The source was placed at the bottom and its length was varied from 1/5 to 1/4 of the total face length. They concluded that bigger sources implied in better heat transfer characteristics.

Altaç and Kurtul (2007) studied a rectangular enclosure with a heat source placed at its center and determined the heat transfer characteristics varying the enclosure inclination angle. Their results showed a maximum Nusselt number for a 22°inclination angle when considering a square enclosure. A different behavior was found when an enclosure with aspect ratio of 2 was simulated. In this case, the Nusselt number was constant up to a 22° inclination and decreased for a higher angle.

Varol et al (2009) analyzed the aspect ratio and inclination effects on the heat transfer in a rectangular enclosure with different boundary conditions. They reported that the heat transfer at the enclosure top was greatly influenced by the inclination.

For natural convection in pin fin arrays the available information is much more restrict. Yu and Joshi (2002) presented a numerical and experimental study considering a rectangular enclosure with a heat source associated to a pin fin sink. The effects of both natural convection and radiation heat transfer were taken into account. They concluded that the radiation plays a very important role at the global heat transfer. Also placing the source at the bottom surface, horizontal orientation, provides a better heat transfer if compared to the source mounted at the vertical wall.

In the present work, the mixed convection inside a rectangular enclosure with a pin-fin array heat sink was considered. A computational procedure for simulating the flow and heat transfer was developed and the influence of aspect ratio, dissipated heat and injected mass was investigated. As a result, the variations on the Nusselt number, based on the overall heat transfer coefficient, as function of the Rayleigh and modified Richardson numbers were calculated.

2. MATHEMATICAL AND NUMERICAL MODELS

The basic geometry considered in this work was similar to that used by Yu and Joshi (2002) and schematized in Fig. 1. Two openings were placed one at the enclosure base and the other at the top surface and fluid injection was imposed at the base wall. The heating element is considered to be inserted at the enclosure wall so that the fin was laid on the internal wall surface.

The developed mathematical model considers conduction in all solid components and steady laminar mixed convection inside the enclosure under the Boussinesq approximation. As pointed out by Yu and Joshi (2002), modeling each pin individually increases the computational domain making it intractable. They proposed, based on the work of Heindel et al. (1996), to treat the finned heat sink as a porous medium and the same approximation was considered here.

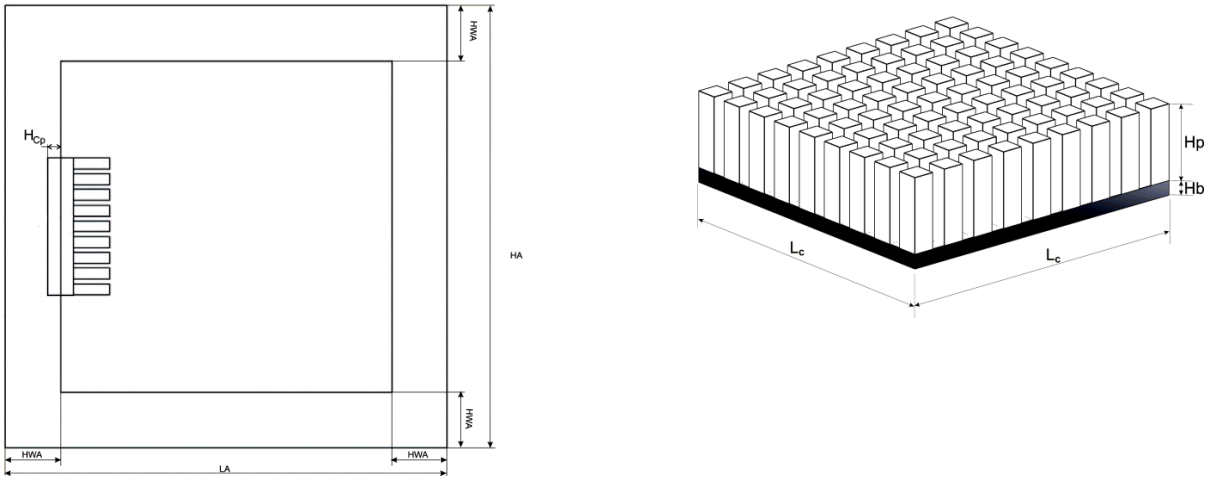

Figure 1 – Enclosure Geometry

2.1. Mathematical Formulation

The modeling for the flow and heat transfer inside the enclosure was performed using the mass, momentum and energy conservation equations. Inside porous medium, since the porosity is normally high in finned heat sinks, a non Darcy model becomes more suitable (Yu and Joshi, 2002). Thus, the Brinkman-Forchheimer model was chosen and local thermal equilibrium between the fluid and the fins was assumed.

In order to write the governing equations the following dimensionless transformations were applied :

$$x^* = \frac{x}{L_c},\ y^* = \frac{y}{L_c},\ p^* = \frac{p}{\rho_f U_0^2},\ \theta = \frac{T - T_c}{T_r},\ u^* = \frac{u}{U_0},\ v^* = \frac{v}{U_0} \tag{1}$$

with

$$U_0 = \left(\frac{g \beta \dot{q} L_c^2 H_c}{k_f} \right)^{1/2} \tag{2}$$

$$T_r = \frac{\dot{q} L_c H_c}{k_f} \tag{3}$$

where l_c and h_c are the component length and height respectively, $\dot{q}$ is the volumetric dissipated heat, and β, k_f and ρ_f are the thermal volumetric expansion coefficient, and the fluid thermal conductivity and density respectively.

The dimensionless governing equations for the whole enclosure are then:

- Mass conservation (fluid and porous media)

$$\frac{\partial u^*}{\partial x^*} + \frac{\partial v^*}{\partial y^*} = 0 \tag{4}$$

- Momentum

-for the fluid

$$\frac{\partial u^* . u^*}{\partial x^*} + \frac{\partial u^* . v^*}{\partial y^*} = \frac{-\partial P^*}{\partial x^*} + \left[\frac{\partial}{\partial x^*} \left(\frac{\mathrm{Pr}}{Ra} \right)^{1/2} \frac{\partial u^*}{\partial x^*} + \frac{\partial}{\partial y^*} \left(\frac{\mathrm{Pr}}{Ra} \right)^{1/2} \frac{\partial u^*}{\partial y^*} \right] \tag{5}$$

$$\frac{\partial u^*.v^*}{\partial x^*}+\frac{\partial v^*.v^*}{\partial y^*}=\frac{-\partial P^*}{\partial y^*}+\left[\frac{\partial}{\partial x^*}\left(\frac{\mathrm{Pr}}{Ra}\right)^{1/2}\frac{\partial v*}{\partial x^*}+\frac{\partial}{\partial y^*}\left(\frac{\mathrm{Pr}}{Ra}\right)^{1/2}\frac{\partial v*}{\partial y^*}\right] \tag{6}$$

- for the pin fin array

$$\frac{1}{\delta^2}\frac{\partial u^*.u^*}{\partial x^*}+\frac{\partial u^*.v^*}{\partial y^*}=\frac{-\partial P^*}{\partial x^*}+\frac{1}{\delta}\left[\frac{\partial}{\partial x^*}\left(\frac{\mathrm{Pr}}{Ra}\right)^{1/2}\frac{\partial u*}{\partial x^*}+\frac{\partial}{\partial y^*}\left(\frac{\mathrm{Pr}}{Ra}\right)^{1/2}\frac{\partial u*}{\partial y^*}\right]+S_x \tag{7}$$

$$\frac{1}{\delta^2}\frac{\partial u^*.v^*}{\partial x^*}+\frac{\partial v^*.v^*}{\partial y^*}=\frac{-\partial P^*}{\partial x^*}+\frac{1}{\delta}\left[\frac{\partial}{\partial x^*}\left(\frac{\mathrm{Pr}}{Ra}\right)^{1/2}\frac{\partial v*}{\partial x^*}+\frac{\partial}{\partial y^*}\left(\frac{\mathrm{Pr}}{Ra}\right)^{1/2}\frac{\partial v*}{\partial y^*}\right]+S_y \tag{8}$$

with

$$S_x=-\frac{1}{Da}.\left(\frac{\mathrm{Pr}}{Ra}\right)^{1/2}u^*-\frac{C}{\sqrt{Da}}.\left|V^*\right|u^* \tag{9}$$

$$S_y=-\frac{1}{Da}.\left(\frac{\mathrm{Pr}}{Ra}\right)^{1/2}v^*-\frac{C}{\sqrt{Da}}.\left|V^*\right|v^*+\theta \tag{10}$$

In these equations, δ is the porosity and C the Forchheimer parameter.

- Energy (all regions)

$$\frac{\partial u^*\theta}{\partial x^*}+\frac{\partial v^*\theta}{\partial y^*}=\left[\frac{\partial}{\partial x^*}\Gamma_j\frac{\partial\theta}{\partial x^*}+\frac{\partial}{\partial y^*}\Gamma_j\frac{\partial\theta}{\partial y^*}\right]+S_q \tag{11}$$

where: $S_q=0$ for the enclosure walls, porous media and fin base and

$S_q=\frac{1}{H_c}\left(\frac{1}{\mathrm{Pr}\,Ra}\right)^{1/2}$ for the heating element. The diffusion coefficient is defined as:

$$\Gamma_j=\frac{k_j}{k_f}\frac{1}{(Ra\,\mathrm{Pr})^{1/2}} \tag{12}$$

with k_j the thermal conductivity of the considered region.

The pin fin array is considered a homogeneous porous media but with different thermal conductivity for both directions. The effective coefficient was evaluated using a series-parallel thermal resistance model.

The dimensionless numbers that result from the normalization process are the Prandtl, Rayleigh and Darcy numbers defined as:

$$\mathrm{Pr}=\frac{\nu}{\alpha} \tag{13}$$

$$Ra=\frac{g.\beta.\dot{q}\,L_c^4\,H_c}{k_f.\alpha.\nu} \tag{14}$$

$$Da=\frac{K}{L_c^2} \tag{15}$$

where the porous medium permeability K was evaluated using the model suggested by Kaviany (1991) for the flow around a bundle of cylinders:

$$\frac{K}{d_h^2} = 0{,}0606\,\frac{\pi}{4}\,\frac{\delta^{5,1}}{1-\delta} \quad for\ 0{,}4 \le \delta \le 0{,}8 \tag{16}$$

with d_h representing the fin hydraulic diameter.

The Forchheimer parameter, C, appearing in Eqs (9) and (10) depends on the porous media configuration. In this work, the value C=0.55 experimentally obtained by Ward (1964) was adopted as a constant.

To complete the mathematical model the boundary conditions must be defined. At all solid surfaces non slip and impervious wall conditions were adopted for the fluid flow. The external wall surface of the side where the component is attached was supposed adiabatic and for the other faces a prescribed constant temperature T_c was adopted.

Mass is injected at the base window with a constant velocity u_o. The normalized velocity is expressed by Eq. (17) and an injection Reynolds number could be defined.

$$v^* = \left(\frac{\mathrm{Pr}}{Ra}\right)^{1/2} \frac{L_c\, u_o}{\nu} = \left(\frac{\mathrm{Re}^2\,\mathrm{Pr}}{Ra}\right)^{1/2} \tag{17}$$

The enclosure outflow is determined using the global mass balance and an upwind scheme.

2.2. Numerical Procedure

A Power-Law differencing scheme was used to transform the differential equations in algebraic system sets. The velocity-pressure coupling was performed by the SIMPLE algorithm detailed by Patankar (1980).

The algebraic equations were solved with an iterative segregated procedure and the Bi-CGSTAB algorithm, proposed by Van der Vorst (1992), was chosen for the computations.

The control volume distribution was done such that only complete and homogeneous volumes for p and T occurred. Staggered grids for u and v velocity components were defined and in this case it was not possible to avoid different materials inside the same volume. In order to guarantee the heat and momentum flux continuity, effective properties must be defined at the control volume faces. Series and parallel resistance network arrangements were considered for this purpose.

A uniform grid of 110x50 nodes was defined after some grid independence tests. The numerical solution was accepted to be converged when the mean Euclidian norm for all the solved systems satisfied the condition:

$$\overline{R} = \frac{\sqrt{\sum_{i=1}^{m} R_i^2}}{m} \le \varepsilon \tag{18}$$

where R_i is the residual value for each discrete equation and m is the number of equations in each set.

The convergence parameter ε was assumed as 10^{-7} for velocity and pressure equations and 10^{-5} for the temperature. Also, the maximum residual for each system should be less than ten times the convergence parameter.

2.3. Model Validation

The developed computational procedure was extensively tested with numerical results found in the literature. First a differentially heated cavity, with opposed hot and cold vertical walls was simulated. Only natural convection heat transfer was taken into account and the results were compared to those reported by Mallinson and Vahl Davis (1977). As a 2D model was used here, the solution for the medium plane was considered for comparison. Also, the works from Deng et al (2002) dealing with discrete wall heat sources and Sathiyamoorthy et al (2007) with linear side wall heating were reproduced.

Finally, taking a unitary porosity, the procedure was tested with the work from Madhavan and Sastri (2000) considering conduction-convection combined process for a box with protuberant heat sources. In all cases the maximum achieved differences for temperature and maximum velocities were within a 3% range.

A direct comparison with Yu and Joshi (2002) was not possible since the present model does not include radiation processes. However, the reported cases for which natural convection played a more important role than radiation were used for a qualitative analysis. The order of magnitude of the calculated Nusselt numbers were compatible with their results.

3. RESULTS

In this section, the obtained results are presented and discussed pointing the main aspects of the heat transfer inside the enclosure. In order to use the same comparison parameter, a Nusselt number was defined. Since there are many different heat transfer processes involved, an overall heat transfer coefficient relating the total heat transferred and the maximum temperature achieved inside the cavity was proposed. Supposing that the total heat transferred could be calculated by:

$$q = U\,A\left(T_{max} - T_c\right) \tag{19}$$

it is possible to define a global Nusselt number by performing the dimensionless transformation of this equation. The resultant expression is:

$$Nu = \frac{U\,L_c}{k_f} = \frac{1}{\theta_{max}} \tag{20}$$

Other used parameter was the Richardson number, that indicates the relative importance of natural and mixed convection for the heat transfer process. In this paper, the used definition for this parameter was:

$$Ri = \frac{Ra}{\mathrm{Re}^2} \tag{21}$$

The geometric dimensionless characteristics of the basic cavity were that detailed in Tab (1) for an enclosure with aspect ratio of 0.5. When the aspect ratio is changed, all the dimensions are kept unchanged except the enclosure length L^*.

Table 1 – Geometric Enclosure Characteristics

Enclosure		Pin-fin array	
Parameter	value	Parameter	Value
L^*	5.0	H_p^*	0.22
H^*	2.5	H_b^*	0.07
H_c^*	0.034	δ	0.72
H_w^*	0.25	k_m/k_f	6850
k_w/k_f	7.4		

The Fig. (2) represents the Nusselt number variations as a function of Rayleigh and Richardson numbers for a 0.5 aspect ratio enclosure.

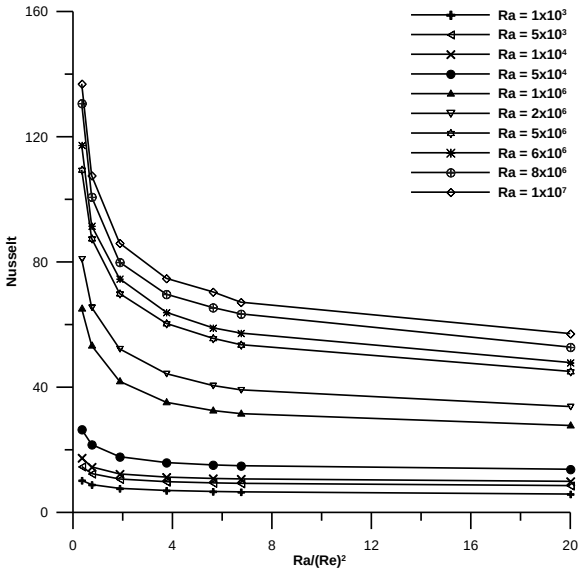

Figure 2. Nusselt number distribution for 0.5 aspect ratio enclosure

All the curves have the same behavior, and the heat transfer is more effective when the forced convection plays important role. Figs. (3) and (4) present, for Ra = 10^3 and 10^6 respectively, the isotherm and streamline distributions for Ri = 20 , 3.75 and 0.35. It can be noted that for lower Reynolds numbers natural and forced convection are important and there is a tendency of some stratification inside the enclosure. When the injected mass increases the heat transfer occurs mainly in a vertical region close to the heat source and most of the cavity stays in a low temperature. The recirculation cells are of low velocity, mainly induced by the forced flow.

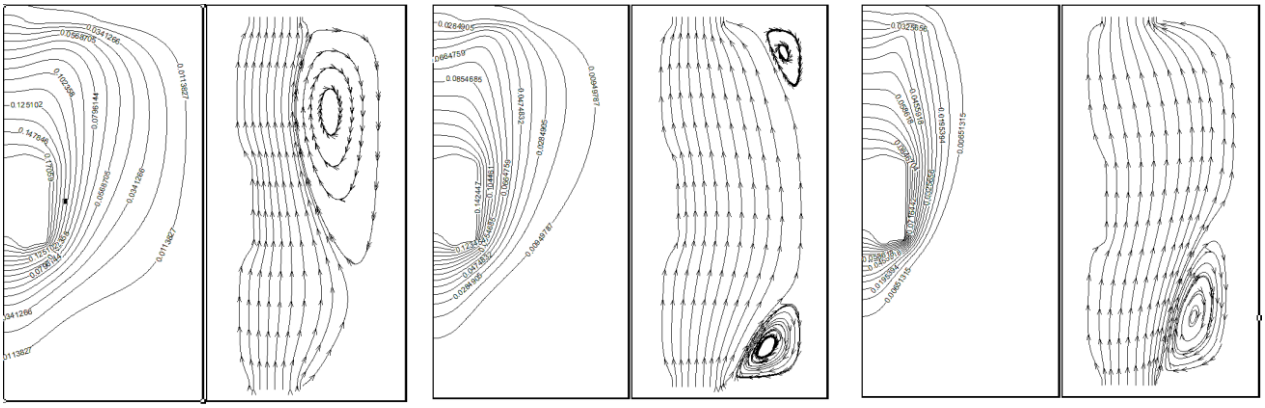

Figure 3 Isotherms and streamlines for Ra = 10^3 and Ri = 20, 3.75 and 0.35

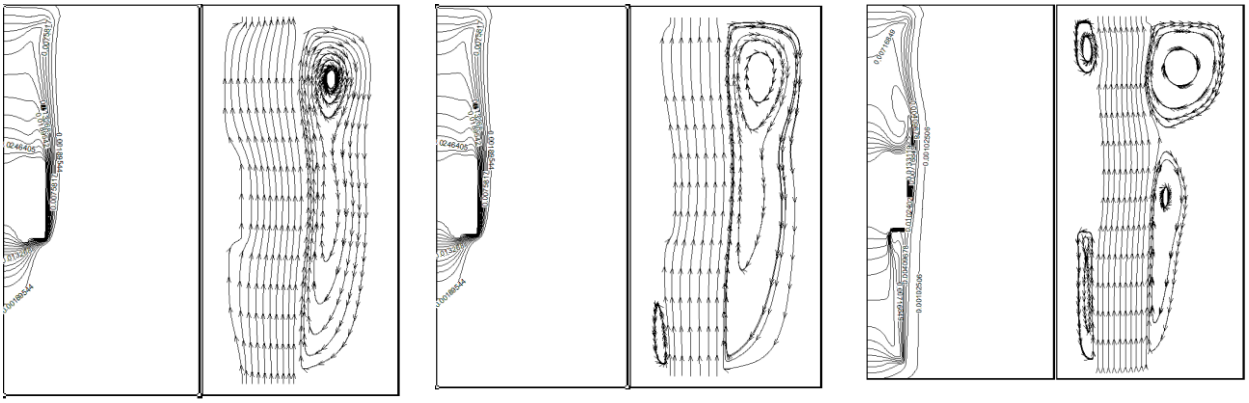

Figure 4- Isotherms and streamlines for Ra = 10^6 and Ri = 20, 3.75 and 0.35

When the aspect ratio is set as 0.6 no great variations are encountered and this fact is corroborated be the behavior of the Nusselt distribution showed in Fig. (5).

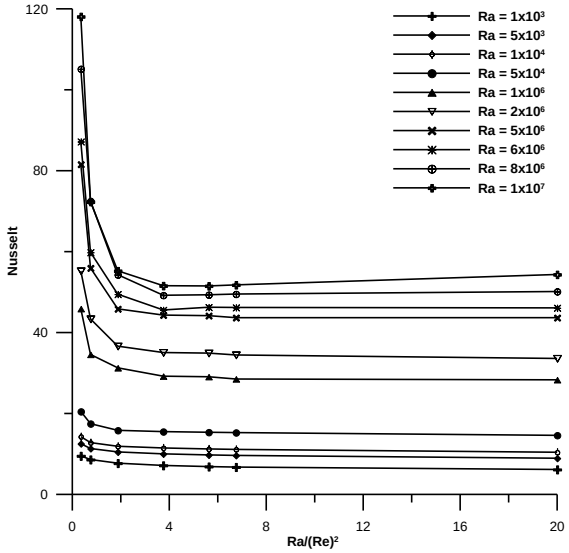

Figure 5. Nusselt number distribution for 0.6 aspect ratio enclosure

Finally, an enclosure with aspect ratio equal to 1.0 was simulated and the Nusselt distribution is represented in Fig 6. As can be verified there is an unexpected inflexion for intermediate values of the Richardson number

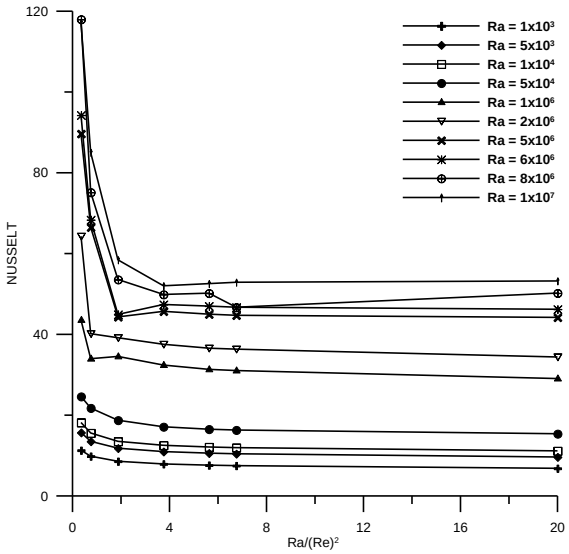

Figure 6. Nusselt number distribution for 1.0 aspect ratio enclosure

Figure (7) represents the isotherms and streamlines for Ra = 10^3. In this case the behavior is similar to the previous cases. For high Richardson number natural convection prevails and a great circulation cell is formed inside the cavity.

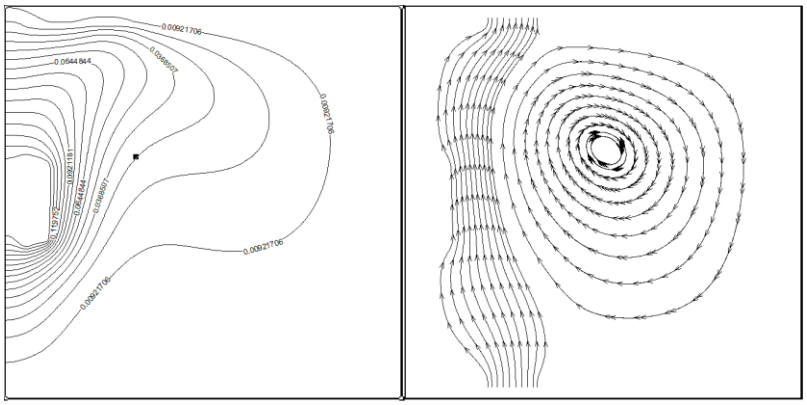

Ri=20

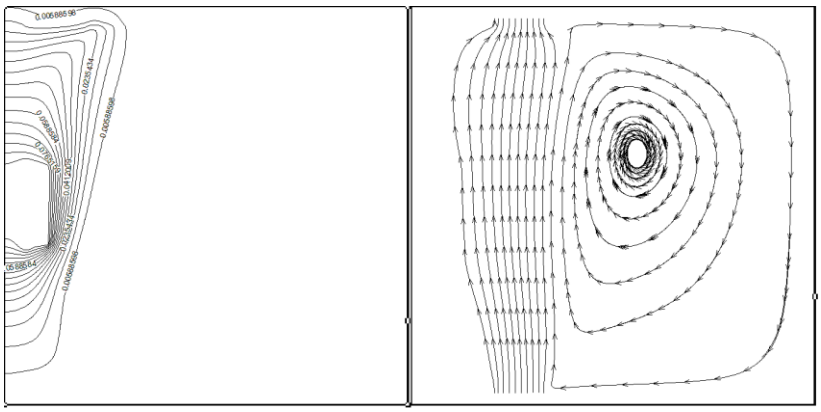

Ri = 0,35

Figure 7 - Isotherms and streamlines for Ra = 10^3 and Ri = 20, and 0.35

Figure (8) presents the results for Ra = $5x10^6$. For high Richardson number natural convection prevails and a great circulation cell is formed inside the cavity. However. when the injected mass increases, initially there is a formation of a recirculation cell near the source base and the forced flow is partially deviated increasing the heat transfer resistance. If the injection velocity is higher, this cell tends to be compressed against the wall and the heat transfer by forced convection prevails.

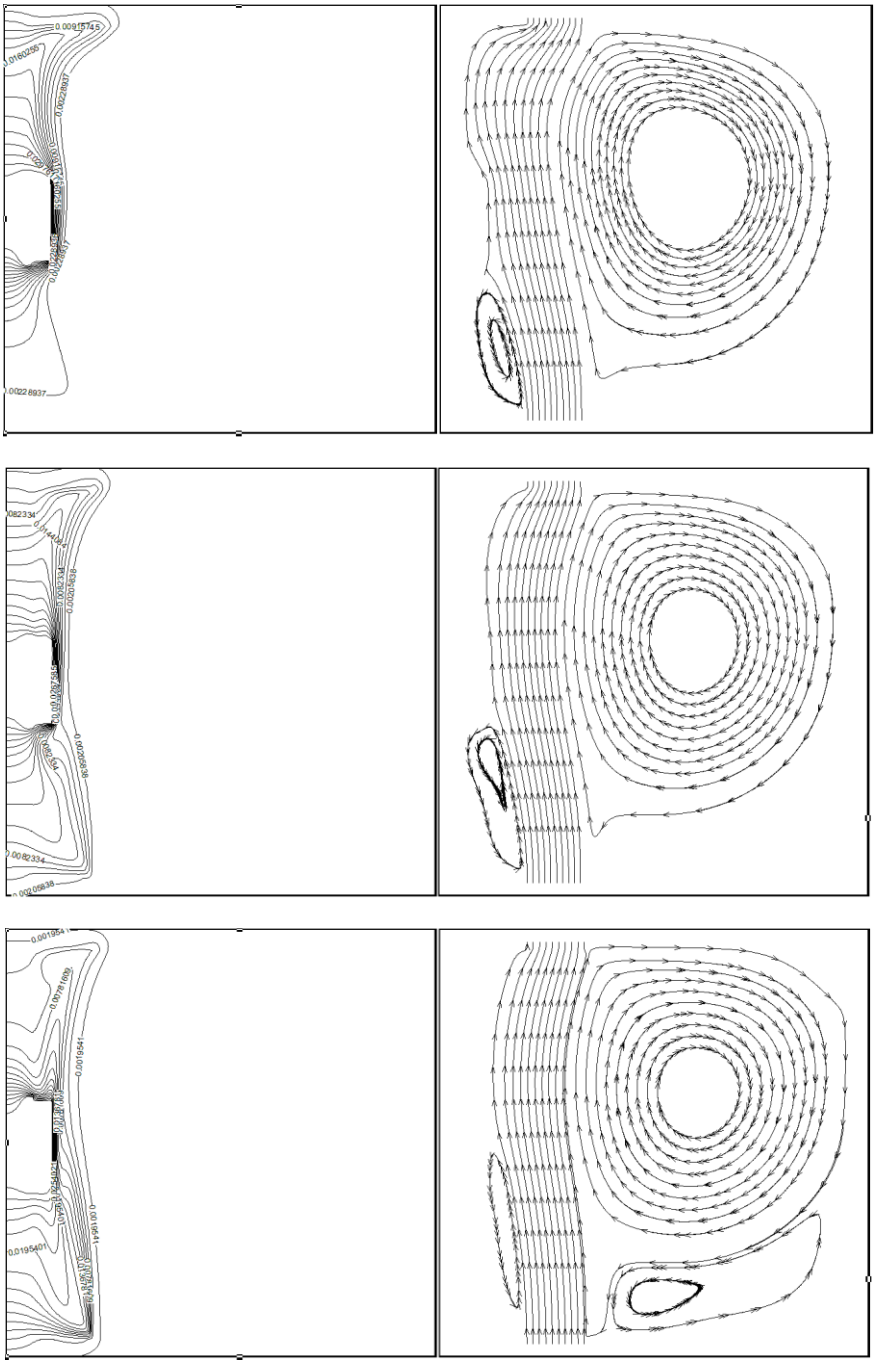

Figure 8 - Isotherms and streamlines for Ra = $5x10^6$ and Ri = 20, 3.75 and 0.35

4. CONCLUSIONS

The heat transfer inside an enclosure with a discrete pin-fin heat sink was studied considering a mixed convection heat transfer process. For the sake of numerical simplicity, the pin-fin array was treated as a porous media using the Brinkman-Forchheimer model.

A numerical procedure was developed and the mass injection rate and the enclosure aspect ratio influences on heat transfer were analyzed.

For small aspect ratio enclosures, the enhancement in the overall heat transfer coefficient was significant when a forced flow is imposed. This behavior was also verified for large aspect ratios, except in a small Richardson range. In this case, a recirculation cell at the heat sink base was formed and this cell, for a small range of Reynolds number, tends to keep the forced flow away from the heat source, and consequently the heat transfer decreased. Intensification on mass injection, represented by a low Richardson number, causes the compression of this cell against the enclosure wall and this phenomena is inhibited. Consequently, the heat transfer increases again.

5. REFERENCES

Altaç, Z., Kurtul, O., 2007. "Natural Convection in Tilted Rectangular Enclosures with a Vertically Situated Hot Plate Inside", Applied Thermal Engineering, Vol. 27, pp. 1832-1840.

Calcagni B., Marsili F., Paroncini M., 2005, "Natural Convective Heat Transfer in Square Enclosures Heated From Below." Applied Thermal Engineering, Vol. 25, pp. 2522-2531.

Deng, Q. H., Tang G. F., Li, Y., 2002, "A Combined Temperature Scale for Analyzing Natural Convection in Rectangular Enclosures with Discrete Wall Heat Sources", Int. J. Heat Mass Transfer, Vol. 45, pp. 3437-3446.

Heindel, T.J., Incropera, F.P., Ramadhyani,S.,1996, "Enhancement of Natural Convection Heat Transfer from an Array of Discrete Heat Sources", Int. J. Heat Mass Transfer, Vol. 39, pp. 479-490.

Kaviani, M., 1991, "Principles of Heat Transfer in Porous Media", Springer-Verlag, New York.

Kraus, A.D., Bar-Cohen, A., 1995, "Design and Analysis of Heat Sinks", John Wiley & Sons, New York.

Madhavan, P. N., Sastri, V. M. K., 2000, "Conjugate Natural Convection Cooling of Protruding Heat Sources Mounted on a Substrate Placed Inside an Enclosure: a Parametric Study", Comput. Methods in Appl. Mech. Eng., Vol. 188, pp. 187-202.

Mallinson, G.D., Vahl Davis, G., 1977, "Three-Dimensional Natural Convection in a Box, a Numerical Study", J. Fluid Mech., Vol. 83, pp. 1-31.

Patankar, S.V., 1980, "Numerical Heat Transfer and Fluid Flow", Hemisphere, New York.

Sathiyamoorthy, M., Basak, T., Roy, S., Pop, I., 2007, "Steady Natural Convection Flows in a Square Cavity with Linearly Heated Side Wall(s)", Int. J. Heat Mass Transfer, Vol. 50, pp. 766-775.

Van Der Vorst, H.A., 1992, "BI-CGSTAB : a Fast and Smoothly Converging Variant of BI-CG for the Solution of Non-Symmetric Linear Systems, SIAM J. Sci. Stat. Comput., Vol. 13, pp. 631-644.

Varol, Y., Oztop H. F., Koca, A., Ozgen, F., 2009, "Natural Convection and Fluid Flow in Inclined Enclosure with a Corner Heater", Applied Thermal Engineering, Vol. 29, pp. 340-350.

Ward, J.C., 1964, "Turbulent flow in porous media", J. Hydraul. Div. ASCE, Vol. 90, pp. 1-12.

Yu, E., Joshi, Y., 2002, "Heat Transfer Enhancement from Enclosed Discrete Components Using Pin-Fin Heat Sinks. Int. J. Heat Mass Transfer, Vo. 45, pp. 4957-4966

6. RESPONSIBILITY NOTICE

The authors are the only responsible for the printed material included in this paper.